Joint Frequency Offset and Channel Estimation for NB-IoT Systems

Pinchang Zhang[1], Ji He[2], Jiankuo Dong[1], Letian Sha[1]

[1]College of Computer, Nanjing University of Posts and Telecommunications, Nanjing, Jiangsu 210028, China

[2]School of Computer Science, Xidian University, Xi'an, Shaanxi, 710071, China (e-mail: jihe@xidian.edu.cn)

The nonlinear distortions resulting from the radio frequency (RF) impairments such as frequency offset, I/Q-imbalance, phase noise, and quantization errors. The hardware impairments severely degrade signal reception performance in NB-IoT systems and hence estimation for hardware impairments is necessary and mitigated by compensation algorithms. To this end, this paper focuses on the problem of estimating channel gains and frequency offsets in an NB-IoT system. Specifically, we first separate channel gains and frequency offsets and derive the analytical expressions of interest, based on the maximum likelihood estimation; We derive the expectation-maximization algorithm and apply it to the NB-IoT system for solving joint estimation of frequency offsets and channel gains; We carry out extensive simulations to illustrate that how systems parameters (e.g., channel phase difference, frequency offset difference, SNR, the number of sampling) can affect estimation performance.

Index Terms—**Narrowband–Internet of Things (NB-IoT), channel gain, frequency offset, Craḿe-Rao Bound (CRB).**

I. INTRODUCTION

THE Internet of Things (IoT) aims at connecting different kinds of objects to the Internet, which is widely applied to in many fields such as e-health care, monitor environments, smart home, smart mobility, and so on [1]. The number and variety of IoT devices have rapidly increased in recent years, for a predictable future of over 60 billions IoT devices access to the Internet by 2025 [2]. Lots of IoT devices are connected by using short-range communication technologies, such as Zigbee, RFID, Bluetooth, and so on. Recent, narrowband IoT (NB-IoT) has been attracted for serving as a low-power wide-area networks (LPWAN) communication standard to achieve interconnection between IoT devices requiring small data volume amounts, low bandwidth, and long battery life [3]. The development of NB-IoT greatly promotes the application of intelligent IoTs, making eligible IoT equipments access to 5G, 6G and beyond networks securely. In addition, NB-IoT exhibits important advantages to provide numerous device connections, information security exchange, highly dynamic device joining/leaving the network, more wide application scenarios.

It is noticed, however that these NB-IoT advantages depend on accurate channel state information and frequency offset to allow for information recovery. Similar to other wideband-based techniques, NB-IoT system is significantly sensitive to frequency offsets induced by oscillator mismatches and/or Doppler shifts. It is proved that a small frequency offset leads to severe degradation in modulation due to suffering from inter-carrier interference and attenuates the desired signal [4]. This will reduce the effective signal-to-noise ratio (SNR) for signal reception and thus degrades NB-IoT system performance. Therefore, it is necessary to estimate the channel gains and the frequency offsets and then compensates for them for NB-IoT system performance impairment. Joint estimation of channel gains and the frequency offsets for NB-IoT system

needs to be unexplored. The objective of this paper is to fill this gap.

Recently, many works have devoted to estimating channels and/or frequency offsets [5]–[7]. The authors in [8] comprehensively explore the problem of joint estimation of the frequency offsets and channels in multi-input multi-output (MIMO) systems using a training sequence, and they analytically derive Craḿe-Rao Bound (CRB) in terms of frequency offsets and channels under maximum likelihood estimator (MLE). In order to reduce the difficulty of n-dimensional maximization problem, the authors in [9] propose two computationally efficient iterative estimation algorithms for joint channel and frequency offset estimation in MIMO systems, namely expectation conditional maximization and space-alternating generalized expectation-maximization. Numerical results illustrate that the proposed two algorithms can achieve the CRB. The authors in [10] focus on joint carrier frequency offset (CFO) and channel estimation in multiuser MIMO orthogonal frequency-division multiplexing (OFDM) systems, and also design optimal training sequences minimizing the CRBs for CFO and channel. Taking into account high-mobility situations MIMO-OFDM access systems [11], two novel approaches for joint CFO and doubly selective channel estimation are developed based on Schmidt–Kalman filtering (SKF) and simulation results demonstrate that the highly increase the mean-square error performance. Channel and CFO estimation at millimeter wave carrier frequencies faces large challenging.

By using a low dimensional equivalent channel matrix, the authors in [12] develop a new approach to estimate the CFO with power amplifier impairment in the time domain in the hybrid mmWave MIMO OFDM systems. Then, by utilizing the sparse nature of mmWave channels in the angle-delay domain and compressibility of the phase error vector, a method for joint CFO and wideband channel estimation algorithm is designed in one-bit receivers in [13]. To overcome the two successive beacons problems, the authors in [14] CFO-robust compressive scanning path-tracking algorithm is presented to enhance the path tracking efficiency of mmWave systems.

These existing approaches mainly focus on MINO, MINO OFDM, and mmWave MINO systems and can not be extended to NB-IoT systems due to different hardware architectures. To comprehensively solve the problem of joint estimation of CFO and channel gains, this paper focuses on exploring joint estimation of CFO and channel gains for NB-IoT systems. The main contributions of this paper are summarized as follows:

- Through statistic signal analysis theory, we first use the separable model to extract channel gain and frequency offset, derive the analytical expressions for channel gain and frequency offset estimation in a NB-IoT system, and then we present CRB for the two estimation, based on the maximum likelihood estimation.
- With the help of tool for signal separable model, we derive the expectation–maximization algorithm and apply it to the NB-IoT system for solving the ML problem in terms of joint estimation of frequency offsets and channel gains.
- Through extensive simulations, we further examine how systems parameters (e.g., channel phase difference, frequency offset difference, SNR, the number of sampling) can affect estimation performance. In addition, we also illustrate that the efficiency of expectation–maximization algorithm for estimating frequency offsets and channel gains the NB-IoT system.

The rest of the paper is organized as follows. Section II gives system model. Section III presents CRB for the estimation parameters. The joint estimation algorithm is presented in Section IV. Finally, Section VI concludes this paper.

Notation: $(\cdot)^*$, $(\cdot)^T$, and $(\cdot)^H$ denote conjugate, transpose, and conjugate transpose operators, respectively. $|\cdot|$ denotes absolute value operator. $\|\mathbf{x}\|$ denotes L_2-norm of a vector $\mathbf{x}$. $\mathbb{C}^{M \times N}$ represents the set of complex-valued $M \times N$ matrices. A circularly symmetric complex Gaussian random vector $\mathbf{x}$ with zero mean and covariance matrix $\mathbf{C}$ can be denoted by $\mathbf{x} \sim \mathcal{CN}(\mathbf{0}, \mathbf{C})$. $\mathbb{E}\{\cdot\}$ and $f(\cdot)$ represent expectation and probability operators, respectively.

II. SYSTEM MODEL

We consider a flat and block-fading NB-IoT system with an M-antenna base station transmitting data streams to a single-antennan NB-IoT device. It is noticed that the received signals always suffer from being distorted by frequency offsets caused by mobility-induced Doppler frequency shift and oscillator mismatch. Therefore, in the presence of frequency offsets the discrete-time baseband received signal model under K observation can be expressed by

$$y(k) = \sum_{m=1}^{M} h_m e^{jw_m k} s_m(k) + n(k), \quad k = 1, 2, ..., K. \quad (1)$$

- $s_m(k)$ is the kth sample symbol that corresponds to the mth transmit antenna and consists of both pilots (known) and data symbols;
- h_m denotes the baseband complex channel coefficient from the mth transmit antenna at the base station to the receive antenna at IoT device. We assume that $\{h_m\}$

are deterministic unknown and remain constant over the interval $[1, 2, ..., K]$;
- w_m is the carrier frequency offset from the mth transmit antenna at the base station to the receive antenna at IoT device. w_m does not change over the interval $[1, 2, ..., K]$ but varies randomly over blocks in time;
- $n(k)$ is the zero-mean complex additive white Gaussian noise (AWGN) with variance σ_n^2, i.e., $n(k) \sim \mathcal{CN}(0, \sigma_n^2)$.

The objective of this paper is to jointly estimate channels and frequency offsets. Here $\{s_m(k)\}_{k=1}^{K}$ are repeatedly used and publicly known. If we define:

- $\mathbf{y} = [y(1) \ y(2) \ \cdots \ y(K)]^T$;
- $\tilde{\mathbf{h}} = [h_1 \ h_2 \ \cdots \ h_M]^T$;
- $\mathbf{w} = [w_1 \ w_2 \ \cdots \ w_M]^T$;
- $\mathbf{x}_m = [x_m(1) \ x_m(2) \ \cdots \ x_m(K)]^T$;
- $\mathbf{e}_m = [e^{jw_m} \ e^{j2w_m} \ \cdots \ e^{jKw_m}]^T$;

Then the received signal vector $\mathbf{y}$ given in (1) can be expressed as

$$\begin{aligned}
\mathbf{y} &= \sum_{m=1}^{M} (\mathbf{x}_m \odot \mathbf{e}_m) h_m + \mathbf{n} \\
&= \sum_{m=1}^{M} \mathbf{x}(w_m) h_m + \mathbf{n} \\
&= \mathbf{X}(\mathbf{w})\tilde{\mathbf{h}} + \mathbf{n}, \quad (2)
\end{aligned}$$

where $\mathbf{n} = [n(1) \ n(2) \ \cdots \ n(K)]^T \sim \mathcal{CN}(\mathbf{0}, \mathbf{R})$; $\mathbf{x}(w_m) = \mathbf{x}_m \odot \mathbf{e}_m \in \mathbb{C}^{K \times 1}$; $\mathbf{X}(\mathbf{w}) = [\mathbf{x}(w_1) \ \mathbf{x}(w_2) \ \cdots \ \mathbf{x}(w_M)] \in \mathbb{C}^{K \times M}$.

III. DERIVATION OF CRAMÉ-RAO BOUND

In this section, we derive the analytical expressions for channel gain and frequency offset estimation, and then we present CRB for the two estimation.

From (2), we know that $\mathbf{y}$ is complex observation vector due to the parameters $\mathbf{h}$, $\mathbf{h}$ and $\mathbf{n}$, and then $\mathbf{y}$ is distributed as

$$\mathbf{y} \sim \mathcal{CN}(\mathbf{X}(\mathbf{w})\tilde{\mathbf{h}}, \mathbf{R}). \quad (3)$$

where $\mathbf{R} = \sigma_n^2 \mathbf{R}_n$. Hence, the probability of the observations is

$$\begin{aligned}
f(\mathbf{y}|\mathbf{w}, \tilde{\mathbf{h}}) &= \frac{1}{\pi^K \det(\mathbf{R})} \\
&\quad \exp\left\{-[\mathbf{Y} - \mathbf{X}(\mathbf{w})\tilde{\mathbf{h}}]^H \mathbf{R}^{-1}[\mathbf{Y} - \mathbf{X}(\mathbf{w})\tilde{\mathbf{h}}]\right\}.
\end{aligned}$$
$$(4)$$

and the log-likelihood function is

$$l(\mathbf{w}, \tilde{\mathbf{h}}; \mathbf{y}) = -[\mathbf{Y} - \mathbf{X}(\mathbf{w})\tilde{\mathbf{h}}]^H \mathbf{R}^{-1}[\mathbf{Y} - \mathbf{X}(\mathbf{w})\mathbf{h}] + \varsigma, \quad (5)$$

where ς does not rely on the parameters to be estimate.

By differentiating $l(\mathbf{w}, \tilde{\mathbf{h}}; \mathbf{y})$ in (5) and setting the result equal to zero, we can obtain the estimate $\tilde{\mathbf{h}}$ as

$$\hat{\tilde{\mathbf{h}}}(\mathbf{y}, \mathbf{w}) = [\mathbf{X}^H(\mathbf{w})\mathbf{X}(\mathbf{w})]^{-1}\mathbf{X}^H(\mathbf{w})\mathbf{y} = \mathbf{X}^\dagger(\mathbf{w})\mathbf{y}, \quad (6)$$

where $\mathbf{X}^{\dagger}(\mathbf{w}) = [\mathbf{X}^H(\mathbf{w})\mathbf{X}(\mathbf{w})]^{-1}\mathbf{X}^H(\mathbf{w})$ is Moore-Penrose pseudo-inverse. Then substituting (6) into (5) yields a compressed log-likelihood function for $\mathbf{w}$:

$$
\begin{aligned}
&l(\mathbf{w}; \mathbf{y}) \\
&= -[\mathbf{y} - \mathbf{X}(\mathbf{w})\mathbf{X}^{\dagger}(\mathbf{w})\mathbf{y}]^H \mathbf{R}^{-1}[\mathbf{y} - \mathbf{X}(\mathbf{w})\mathbf{X}^{\dagger}(\mathbf{w})\mathbf{y}] + \varsigma,
\end{aligned}
\tag{7}
$$

Combining (6) and (7), we find that the projection matrix onto the signal subspace defined by $\mathbf{X}(\mathbf{w})$ is expressed as

$$
\mathbf{P}_{\mathbf{X}(\mathbf{w})} \triangleq \mathbf{X}(\mathbf{w})[\mathbf{X}^H(\mathbf{w})\mathbf{X}(\mathbf{w})]^{-1}\mathbf{X}^H(\mathbf{w}).
\tag{8}
$$

Based on (8), (7) becomes

$$
\begin{aligned}
l(\mathbf{w}; \mathbf{y}) &= -[\mathbf{y} - \mathbf{P}_{\mathbf{X}(\mathbf{w})}\mathbf{y}]^H \mathbf{R}^{-1}[\mathbf{y} - \mathbf{P}_{\mathbf{X}(\mathbf{w})}\mathbf{y}] + \varsigma \\
&= -[\mathbf{P}_{\mathbf{X}(\mathbf{w})}^{\perp}\mathbf{y}]^H \mathbf{R}^{-1}[\mathbf{P}_{\mathbf{X}(\mathbf{w})}^{\perp}\mathbf{y}] + \varsigma,
\end{aligned}
\tag{9}
$$

where $\mathbf{P}_{\mathbf{X}(\mathbf{w})}^{\perp}$ denotes the orthogonal projection matrix of $\mathbf{P}_{\mathbf{X}(\mathbf{w})}$ that does not contain $\mathbf{X}(\mathbf{w})$.

By maximizing $l(\mathbf{w}; \mathbf{y})$ in (9), we can obtain the ML estimate of $\mathbf{w}$ as

$$
\hat{\mathbf{w}} = \arg\max_{\mathbf{w}} \left\{ [\mathbf{P}_{\mathbf{X}(\mathbf{w})}^{\perp}\mathbf{y}]^H \mathbf{R}^{-1}[\mathbf{P}_{\mathbf{X}(\mathbf{w})}^{\perp}\mathbf{y}] \right\}.
\tag{10}
$$

When we acquire the estimate of $\hat{\mathbf{w}}$, we substitute it back into (6) to get $\hat{\tilde{\mathbf{h}}}$, that is,

$$
\hat{\tilde{\mathbf{h}}}(\mathbf{y}) = \mathbf{X}^{\dagger}(\hat{\mathbf{w}})\mathbf{y}.
\tag{11}
$$

In order to derive the CRB, we define $\mathbf{h}$ as a real $2M$ vector form:

$$
\mathbf{h} \triangleq [\Re(\mathbf{h})^T \; \Im(\mathbf{h})^T]^T.
\tag{12}
$$

Using the ML estimate theory, the Fisher information matrix with respect to $\mathbf{J_F}(\mathbf{h})$, $\mathbf{J_F}(\mathbf{h}, \mathbf{w})$, $\mathbf{J_F}(\mathbf{w}, \mathbf{h})$ and $\mathbf{J_F}(\mathbf{w})$ is expressed as

$$
\mathbf{J_F}(\mathbf{h}) = \begin{bmatrix} \mathbf{J_F}(\mathbf{h}) & \mathbf{J_F}(\mathbf{h}, \mathbf{w}) \\ \mathbf{J_F}(\mathbf{w}, \mathbf{h}) & \mathbf{J_F}(\mathbf{w}) \end{bmatrix}.
\tag{13}
$$

Then the Fisher information matrix for $\mathbf{h}$ is given by

$$
\mathbf{J_F}(\mathbf{h}) = \begin{bmatrix} \mathbf{J_F}(\Re(\mathbf{h})) & \mathbf{J_F}(\Re(\mathbf{h}), \Im(\mathbf{h})) \\ \mathbf{J_F}(\Im(\mathbf{h}), \Re(\mathbf{h})) & \mathbf{J_F}(\Im(\mathbf{h})). \end{bmatrix}
\tag{14}
$$

Based on [15], we have

$$
\mathbf{J_F}(\Re(\mathbf{h})) = 2\Re[\mathbf{X}^H(\mathbf{w})\mathbf{R}^{-1}\mathbf{X}(\mathbf{w})],
\tag{15}
$$

$$
\begin{aligned}
\mathbf{J_F}(\Re(\mathbf{h}), \Im(\mathbf{h})) &= 2\Re[\mathbf{X}^H(\mathbf{w})\mathbf{R}^{-1}(j\mathbf{X}(\mathbf{w}))] \\
&= -2\Im[\mathbf{X}^H(\mathbf{w})\mathbf{R}^{-1}\mathbf{X}(\mathbf{w})].
\end{aligned}
\tag{16}
$$

$$
\begin{aligned}
\mathbf{J_F}(\Im(\mathbf{h})) &= 2\Re[(-j\mathbf{X}(\mathbf{w}))^H \mathbf{R}^{-1}(j\mathbf{X}(\mathbf{w}))] \\
&= 2\Re[\mathbf{X}^H(\mathbf{w})\mathbf{R}^{-1}\mathbf{X}(\mathbf{w})],
\end{aligned}
\tag{17}
$$

$$
\mathbf{J_F}(\Im(\mathbf{h}), \Re(\mathbf{h})) = 2\Re[\mathbf{X}^H(\mathbf{w})\mathbf{R}^{-1}(\mathbf{X}(\mathbf{w}))].
\tag{18}
$$

Substituting $\mathbf{J_F}(\Re(\mathbf{h}))$, $\mathbf{J_F}(\Re(\mathbf{h}), \Im(\mathbf{h}))$, $\mathbf{J_F}(\Im(\mathbf{h}))$ and $\mathbf{J_F}(\Im(\mathbf{h}), \Re(\mathbf{h}))$ into (14), we can obtain $\mathbf{J_F}(\mathbf{h})$ as

$$
\mathbf{J_F}(\mathbf{h}) =
$$

$$
\begin{bmatrix} 2\Re[\mathbf{X}^H(\mathbf{w})\mathbf{R}^{-1}\mathbf{X}(\mathbf{w})] & -2\Im[\mathbf{X}^H(\mathbf{w})\mathbf{R}^{-1}\mathbf{X}(\mathbf{w})] \\ 2\Im[\mathbf{X}^H(\mathbf{w})\mathbf{R}^{-1}\mathbf{X}(\mathbf{w})] & 2\Re[\mathbf{X}^H(\mathbf{w})\mathbf{R}^{-1}\mathbf{X}(\mathbf{w})] \end{bmatrix}
\tag{19}
$$

Following a similar manner, $\mathbf{J_F}(\mathbf{h}, \mathbf{w})$ and $\mathbf{J_F}(\mathbf{w})$ are calculated respectively as,

$$
\mathbf{J_F}(\mathbf{h}, \mathbf{w}) = \begin{bmatrix} 2\Re[\mathbf{X}^H(\mathbf{w})\mathbf{R}^{-1}\mathbf{Z}(\mathbf{w})\boldsymbol{\Lambda}] \\ 2\Im[\mathbf{X}^H(\mathbf{w})\mathbf{R}^{-1}\mathbf{Z}(\mathbf{w})\boldsymbol{\Lambda}] \end{bmatrix}
\tag{20}
$$

$$
\mathbf{J_F}(\mathbf{w}) = [2\Re[\boldsymbol{\Lambda}^H \mathbf{Z}^H(\mathbf{w})\mathbf{Z}(\mathbf{w})\boldsymbol{\Lambda}]]
\tag{21}
$$

where

$$
\mathbf{Z}(\mathbf{w}) \triangleq \begin{bmatrix} \dfrac{\partial \mathbf{x}(w_1)}{\partial w_1} & \dfrac{\partial \mathbf{x}(w_2)}{\partial w_2} & \cdots & \dfrac{\partial \mathbf{x}(w_M)}{\partial w_M} \end{bmatrix}
\tag{22}
$$

$$
\boldsymbol{\Lambda} \triangleq \operatorname{diag}(\tilde{\mathbf{h}}) = \begin{bmatrix} h_1 & 0 & \cdots & 0 \\ 0 & h_2 & \cdots & 0 \\ \vdots & \vdots & \ddots & \vdots \\ 0 & 0 & \cdots & h_M \end{bmatrix}.
\tag{23}
$$

By exploiting the formulation for the inverse of a partitioned matrix in [15], we can obtain the CRB for $\mathbf{w}$ as

$$
\begin{aligned}
\operatorname{CRB}(\mathbf{w}) &= \frac{1}{2}\left[\mathbf{J_F}(\mathbf{w}) - \mathbf{J_F}(\mathbf{w}, \mathbf{h})\mathbf{J_F}(\mathbf{h})^{-1}\mathbf{J_F}(\mathbf{h}, \mathbf{w})^{-1} \right]^{-1} \\
&= \left[\Re[\boldsymbol{\Upsilon} \odot \mathbf{H}^T] \right]^{-1},
\end{aligned}
\tag{24}
$$

where

$$
\boldsymbol{\Upsilon} \triangleq \mathbf{Z}^H(\mathbf{w})\mathbf{P}_{\mathbf{X}(\mathbf{w})}^{\perp}\mathbf{R}^{-1}\mathbf{P}_{\mathbf{X}(\mathbf{w})}^{\perp}\mathbf{Z}(\mathbf{w}),
\tag{25}
$$

$$
\mathbf{H} \triangleq \mathbf{h}\mathbf{h}^H.
\tag{26}
$$

Based on (24) and the formulation for the inverse of a partitioned matrix in [15], we can also readily derive the CRB for $\tilde{\mathbf{h}}$ as

$$
\begin{aligned}
\operatorname{CRB}(\tilde{\mathbf{h}}) &= \left[\mathbf{J_F}(\mathbf{h}) - \mathbf{J_F}(\mathbf{h}, \mathbf{w})\mathbf{J_F}(\mathbf{w})^{-1}\mathbf{J_F}(\mathbf{w}, \mathbf{h})^{-1} \right]^{-1} \\
&= \mathbf{X}^H(\mathbf{w})\mathbf{R}^{-1}\mathbf{X}(\mathbf{w}) \\
&\quad + \mathbf{X}^{\dagger}(\mathbf{w})\mathbf{Z}(\mathbf{w})\left[\operatorname{CRB}(\mathbf{w}) \odot \mathbf{H}\right]\mathbf{Z}^H(\mathbf{w})(\mathbf{X}^{\dagger}(\mathbf{w}))^H
\end{aligned}
\tag{27}
$$

Now, it is observed that the CRB for the estimation of $\mathbf{h}$ and $\mathbf{w}$ is governed by all h_ms through the diagonal matrix defined in (23). On the other hand, it also relies on the differences $w_i - w_k$.

IV. PROPOSED JOINT ESTIMATION FOR CHANNEL AND FREQUENCY OFFSETS

In this section, we present the expectation–maximization (EM) algorithm for joint estimation of channels and frequency offsets algorithm in an NB-IoT system.

From the received signal given in (2), we know that the parameters to be estimate include the $M \times 1$ real vector $\mathbf{w}$ and $M \times 1$ complex vector $\tilde{\mathbf{h}}$. Hence, we define

$$
\boldsymbol{\nu} \triangleq [\mathbf{w}^T \; \tilde{\mathbf{h}}^T]^T.
\tag{28}
$$

It is seen from (5) that if we discard constant terms and scale factors, the log-likelihood function in (5) will become

$$
l(\boldsymbol{\nu}; \mathbf{y}) = -[\mathbf{y} - \mathbf{X}(\mathbf{w})\tilde{\mathbf{h}}]^H \mathbf{R}^{-1}[\mathbf{y} - \mathbf{X}(\mathbf{w})\mathbf{h}],
\tag{29}
$$

We know that the observation $\mathbf{y}$ is a incomplete data. In order to achieve a better estimate accuracy, we should choose the

complete data, so it is necessary to use the observation of each component of $\mathbf{X}(\mathbf{w})\tilde{\mathbf{h}}$ by itself in the presence of noise. Therefor, according to (2), we have

$$\mathbf{y}_m = \mathbf{x}(w_m)h_m + \mathbf{n}_m, m = 1, 2, ..., M. \qquad (30)$$

with

$$\mathbb{E}\{\mathbf{n}_m \mathbf{n}_m^H\} = \alpha_m \mathbf{R}, \qquad (31)$$

and

$$\sum_{m=1}^{M} \alpha_m = 1 \qquad (32)$$

Indeed, for simplicity we can define

$$\alpha_m = \frac{1}{M}. \qquad (33)$$

The observation $\mathbf{y}$ is readily expressed as

$$\mathbf{y} = \sum_{m=1}^{M} \mathbf{y}_m$$

$$\triangleq \Phi \begin{bmatrix} \mathbf{y}_1 \\ \mathbf{y}_2 \\ \vdots \\ \mathbf{y}_M \end{bmatrix}. \qquad (34)$$

where $\Phi[\cdots]$ denotes a many-to-one (noninvertible) linear transformation and then $\mathbf{y}$ and $\mathbf{y}_m$ are jointly Gaussian.

Here we denote the estimate of $\boldsymbol{\nu}$ at step i of the iteration by $\hat{\boldsymbol{\nu}}^{(i)}$. If $\mathbf{y}_m$s were available, we would maximize $l(\boldsymbol{\nu}; \mathbf{y})$ given in (29). Since only $\mathbf{y}$ is obtained, we resort to determine the expectation of $l(\boldsymbol{\nu}; \mathbf{y})$, under given the observation $\mathbf{y}$ and the current parameter estimate $\hat{\boldsymbol{\nu}}^{(i)}$. If we define the resulting expectation by $V(\boldsymbol{\nu}; \hat{\boldsymbol{\nu}}^{(i)})$, and then the conditional expectation with respect to $\mathbf{y}$ and $\hat{\boldsymbol{\nu}}^{(i)}$ is given by

$$V(\boldsymbol{\nu}; \hat{\boldsymbol{\nu}}^{(i)}) = V(\hat{\mathbf{w}}, \hat{\tilde{\mathbf{h}}}; \hat{\mathbf{w}}^{(i)}, \hat{\tilde{\mathbf{h}}}^{(i)})$$

$$\triangleq \mathbb{E}\{\ln f(\mathbf{y}_m : \hat{\mathbf{w}}, \hat{\tilde{\mathbf{h}}}|\mathbf{y}, \hat{\mathbf{w}}^{(i)}, \hat{\tilde{\mathbf{h}}}^{(i)}))\}. \qquad (35)$$

Discarding constant terms and scalar factors, the log-likelihood function can be simplified to

$$l(\boldsymbol{\nu}; \mathbf{y}) = -\sum_{m=1}^{M} [\mathbf{y}_m - \mathbf{x}(w)_m h_m]^H \mathbf{R}^{-1} [\mathbf{y}_m - \mathbf{x}(w)_m h_m], \qquad (36)$$

According to [15], we notice that assessing (35) reduces to finding the conditional mean. We utilize Bayes criterion to obtain $f(\mathbf{y}_m|\mathbf{y})$ from $f(\mathbf{y}|\mathbf{y}_m)$ and find the mean by inspection,

$$\hat{\mathbf{y}}_m^{(i)} = \mathbf{x}(\hat{w}_m)^{(i)}\hat{h}_m^{(i)} + \frac{1}{M}\left[\mathbf{y} - \mathbf{X}(\hat{\mathbf{w}})^{(i)}\hat{\mathbf{h}}^{(i)}\right]. \qquad (37)$$

or

$$\hat{\mathbf{y}}_m^{(i)} - \mathbf{x}(\hat{w}_m)^{(i)}\hat{h}_m^{(i)} = \frac{1}{M}\left[\mathbf{y} - \mathbf{X}(\hat{\mathbf{w}})^{(i)}\hat{\mathbf{h}}^{(i)}\right]. \qquad (38)$$
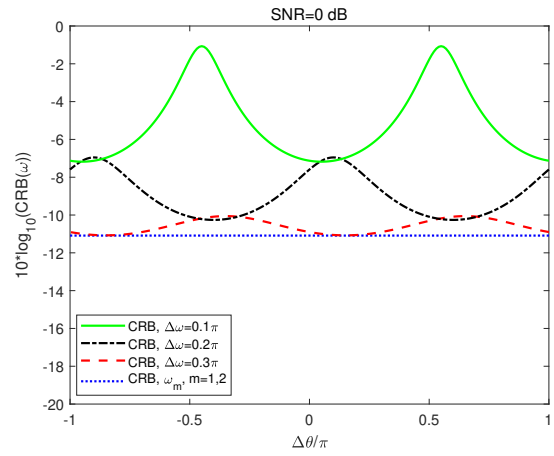
This is called the expectation step.

Fig. 1. Impact of the channel phase difference on CRB for frequency offset.

The next step is to maximize $V(\boldsymbol{\nu}; \hat{\boldsymbol{\nu}}^{(i)})$ with respect to $\hat{\boldsymbol{\nu}}^{(i)}$. The resulting estimate is $\hat{\boldsymbol{\nu}}^{(i+1)}$ and then we have

$$\hat{\boldsymbol{\nu}}^{(i+1)} = \arg\max_{\boldsymbol{\nu}} \left\{V(\boldsymbol{\nu}; \hat{\boldsymbol{\nu}}^{(i)})\right\}. \qquad (39)$$

According to (39), we obtain the estimate of $\mathbf{w}$ and $\tilde{\mathbf{h}}$ as

$$\hat{\mathbf{w}} = \arg\max_{w} \left\{[\mathbf{X}^{\mathbf{H}}(\mathbf{w})\mathbf{R}^{-1}\mathbf{X}^{\mathbf{H}}(\mathbf{w})]^{-1}\mathbf{X}^{\mathbf{H}}(\mathbf{w})\mathbf{R}^{-1}\mathbf{y}\right\}. \qquad (40)$$

and

$$\hat{\tilde{\mathbf{h}}} = \mathbf{X}^{\dagger}(\hat{\mathbf{w}})\mathbf{y}. \qquad (41)$$

The corresponding one-dimensional relation for the complete data is

$$\hat{w}_m^{(i+1)}$$
$$= \arg\max_{w_m} \left\{[\mathbf{x}^H(w_m)\mathbf{R}^{-1}\mathbf{X}^H(w_m)]^{-1}\mathbf{X}^H(w)_m\mathbf{R}^{-1}\hat{\mathbf{y}}_m^{-1}\right\}. \qquad (42)$$
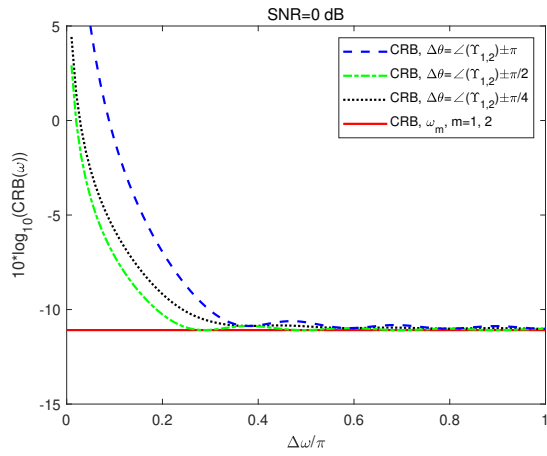
and the one-dimensional version of (41) is

$$\hat{\tilde{h}}_m^{(i+1)} = \mathbf{x}^{\dagger}(\hat{w}_m^{(i+1)})\hat{\mathbf{y}}^{(i)}. \qquad (43)$$

V. NUMERICAL RESULTS

A. System Parameters and Simulation Settings

In our simulation, the number of transmitter and receiver antennas is set to 2 and 1, respectively. We adopt phase-modulated (QPSK) signals generated for pilot symbols. The frequency offsets between the transmitter and receive antennas are set to $\mathbf{w} = [w_1, w_2]^T$ and $w_1, w_2 \in 2\pi[0, 0.3]$. The channels are followed by using zero-mean complex Gaussian distribution with variance 1, and the channels $\tilde{\mathbf{h}} = [h_1 \ h_2]^T = [0.1074 - 0.9303i \ \ 0.2929 + 0.5169i]^T$. The additive noise is the zero-mean complex Gaussian distributed with variance σ_n^2, where we set $\sigma_n^2 = 1/\text{SNR}$ with SNR representing the signal-to-noise ratio. We denote the channel phase difference by $\Delta\theta$ and frequency offset difference by Δw.

Fig. 2. CRB(ω) versus the frequency separation.

Fig. 3. CRB(ω) vs. SNR under different $\Delta\theta$, $N = 5$, $\Delta w = 0.3\pi$.

Fig. 4. CRB(ω) vs. SNR under different $\Delta\theta$, $N = 10$, $\Delta w = 0.3\pi$.

B. Performance Analysis

First, we investigate how the CRB for frequency offset varies with the channel phase difference. To this end, we provide plots of the CRB for the frequency offset vs. the channel phase difference in Fig. 1 with the setting of SNR=0 dB, $N = 10$, and three frequency offsets $\Delta w \in \{0.1\pi, 0.2\pi, 0.3\pi\}$, $\Delta\theta$ varying from $\pi to \pi$. Also, we plot the CRB for estimating w_m for $m = 1, 2$ (the CRBs for w_1 and w_2 are identical). We can see from Fig. 1 that the CRB for estimating w_m remains constant, indicating that the CRB for estimating w_m is not affected by the variation of channel phase difference. We also observe from Fig. 1 that we have the best the CRBs for $\Delta w = 0.1\pi$ or $\Delta w = 0.3\pi$ when the channel phase difference $\Delta\theta = \angle(\Upsilon_{1,2}) \pm \pi/2$, where $\Upsilon_{1,2}$ is the upper right entry in the Υ given in (25). We have the weakest CRBs under this case when $\Delta\theta = \angle(\Upsilon_{1,2}) \pm \pi$. However, when $\Delta w = 0.2\pi$, the opposite is true.

Next, we examine how the frequency separation affects the CRB(ω). In Fig. 2, we present the results that CRB(ω) versus the frequency separation with the setting of SNR=0 dB, $N = 10$, and three channel phase $\Delta\theta \in \{\angle(\Upsilon_{1,2}) \pm \pi, \angle(\Upsilon_{1,2}) \pm \pi/4, \angle(\Upsilon_{1,2}) \pm \pi/2\}$, Δw varying from $0 to \pi$. It is seen from Fig. 2 that the CRB for estimating w_m is not affected by the variation of frequency separation. As shown in Fig. 2, the best CRB(ω) performance occurs when $\Delta\theta = \angle(\Upsilon_{1,2}) \pm \pi/2$, while the worst CRB($\omega$) performance occurs when $\Delta\theta = \angle(\Upsilon_{1,2}) \pm \pi$. This reveals that the channel phase separation $\Delta\theta$ seriously affects CRB(ω) performance as Δw reduces. Another important observation from Fig. 2 is that when the frequency separation reduces, the two-signal CRB will be much larger than the single-signal case, so that it is harder to estimate the frequencies the closer they are.

Now, we explore the impact of SNR on CRB(ω) performance. In Fig. 3 and Fig. 6, we present the plots of CRB(ω) vs. SNR under different $\Delta\theta$, N, Δw. We can see from Fig. 3 and Fig. 6 that the estimation performance of the ML estimator for w gradually decreases as SNR increases. These four figures also exhibits that for a given SNR, the best CRB(ω) performance occurs when $\Delta\theta = \angle(\Upsilon_{1,2}) \pm \pi/2$, and the worst CRB($\omega$) performance occurs when $\Delta\theta = \angle(\Upsilon_{1,2}) \pm \pi$.
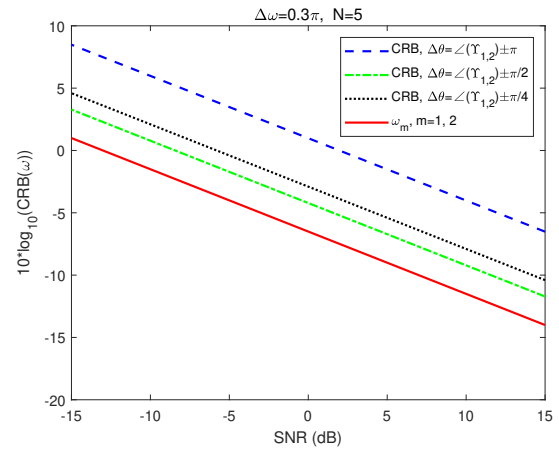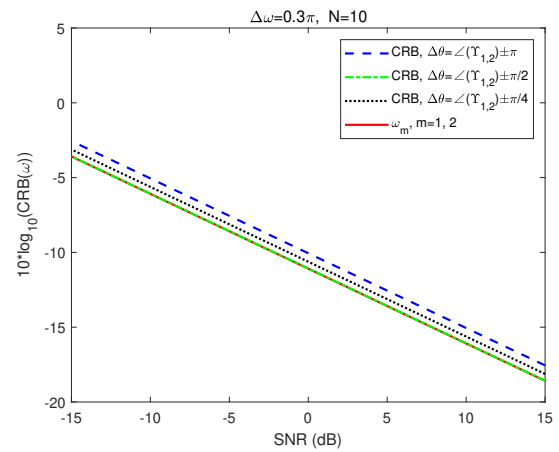
Comparing with Fig. 3 and Fig. 4, we find that for a fixed $\Delta w = 0.3\pi$, the value of N has a significant impact on the CRB(ω) performance. More precisely, when $\Delta w = 0.3\pi$ and $N = 10$, the estimation performance of the ML estimator for w is not sensitive to the change of $\Delta\theta$ while when $\Delta w = 0.3\pi$ and $N = 5$, the estimation performance exhibits disperse under different $\Delta\theta$. In addition, one can see from Fig. 5 and Fig. 6 that for $\Delta w = 0.1\pi$ case, the estimation performance of the ML estimator for w is very sensitive to the change of $\Delta\theta$.

Then, we show that the impact of SNR on CRB(h) performance. To this end, we plot in Fig. 7 and Fig. 8 CRB(h) vs. SNR under different $\Delta\theta$, $N = 10$, Δw. From the two figures, we can see that the estimation performance of the ML estimator for h gradually decreases as SNR increases. It is notable that for a given N, the value of Δw severely affects CRB(h) performance. In particular, when $\Delta w = 0.3\pi$, the estimation performance of the ML estimator for h tends to single h estimation performance, shows a better performance, and is not related to the value of $\Delta\theta$. Moreover, we show in Fig. 9 that estimation algorithm convergence for estimating two ω. Fig. 9 illustrates that the estimation algorithm takes ten iterations to converge estimating two ω.

Finally, it demonstrates in Fig. 10 that frequency offset estimation Root Mean Square Error (RMSE) versus SNR for 2D
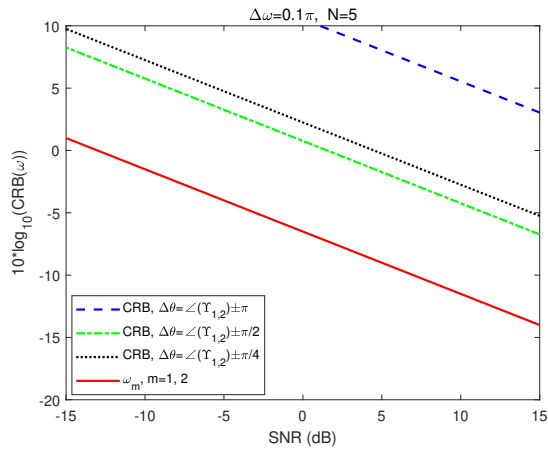
Fig. 5. CRB(ω) vs. SNR under different $\Delta\theta$, $N = 5$, $\Delta w = 0.1\pi$.
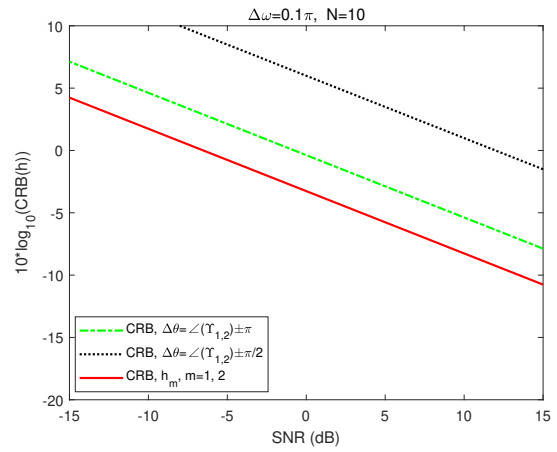
Fig. 7. CRB(h) vs. SNR under different $\Delta\theta$, $N = 10$, $\Delta w = 0.1\pi$.
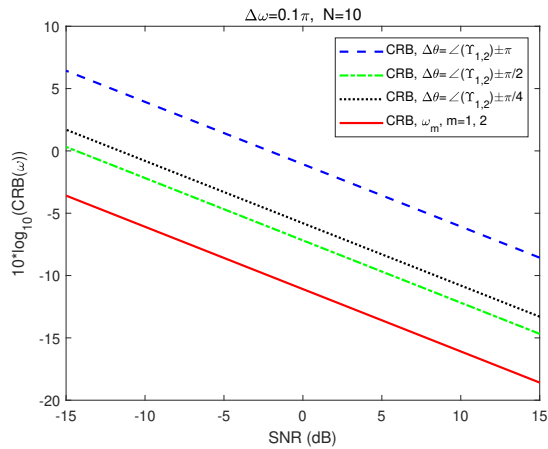
Fig. 6. CRB(ω) vs. SNR under different $\Delta\theta$, $N = 10$, $\Delta w = 0.1\pi$.
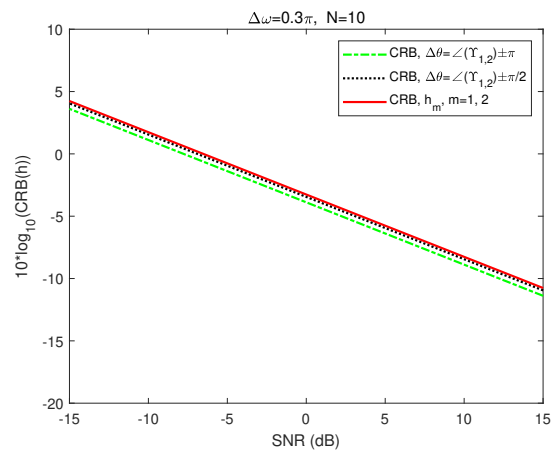
Fig. 8. CRB(h) vs. SNR under different $\Delta\theta$, $N = 10$, $\Delta w = 0.3\pi$.

maximization using EM algorithm under $\Delta\theta = \angle(\Upsilon_{1,2}) \pm \pi$, $N = 10$, $\Delta w = 0.3\pi$. We can observe from Fig. 10 that the SNRs has a large impact on RMSE of ω estimation performance. Specifically, at a low SNR region, it has a performance gap between the RMSE of ω and CRB(ω); at a high SNR region, the RMSE of ω almost approaches to CRB(ω).

VI. CONCLUSION

In this paper, we investigated the problem of joint estimation of channel gains and frequency offsets in an NB-IoT system. We derived the analytical expressions for channel gains and frequency offset estimation under the maximum likelihood estimation. We also presented the expectation–maximization algorithm and apply it to the NB-IoT system for solving joint estimation of frequency offsets and channel gains. Extensive simulation results were provided to show that the impact of systems parameters (such as channel phase difference, frequency offset difference, SNR, the number of sampling) on estimation performance.

ACKNOWLEDGMENT

REFERENCES

[1] D. F. Meneghello, M. Calore, "IoT: Internet of threats? a survey of practical security vulnerabilities in real IoT devices," *IEEE Internet of Things Journal*, vol. 6, no. 5, pp. 8182–8201, Oct. 2019.

[2] Y. S. Dabbagh and W. Saad, "Authentication of wireless devices in the internet of things: Learning and environmental effects," *IEEE Internet of Things Journal*, vol. 6, no. 4, pp. 6692–6705, Aug. 2019.

[3] M. M. J. Cao, P. Yu and W. Gao, "Fast authentication and data transfer scheme for massive NB-IoT devices in 3GPP 5G network," *IEEE Internet of Things Journal*, vol. 6, no. 2, pp. 1561–1575, Apr. 2019.

[4] N. K. M. Wazid, A. K. Das, "Design and analysis of secure lightweight remote user authentication and key agreement scheme in internet of drones deployment," *IEEE Internet of Things Journal*, vol. 6, no. 2, pp. 3572–3584, Apr. 2019.

[5] N. G.-P. J. Rodríguez-Fernández, "Channel estimation for hybrid mmwave MIMO systems with CFO uncertainties," *IEEE Transactions on Wireless Communications*, vol. 18, no. 10, pp. 4636–4652, Oct. 2020.

[6] M. N. A. Brighente, M. Cerutti, "Estimation of wideband dynamic mmwave and THz channels for 5G systems and beyond," *IEEE Journal on Selected Areas in Communications*, vol. 38, no. 9, pp. 2026–2040, Sept. 2020.

[7] A. K. D. M. A. Azam and A. Mukherjee, "Uplink channel estimation with hardware imperfections, antenna position error and channel correlation for nested and linear array antennas," *IEEE Transactions on Vehicular Technology*, vol. 69, no. 12, pp. 15 412–15 426, Dec. 2020.

[8] O. Besson and P. Stoica, "On parameter estimation of MIMO flat-fading channels with frequency offsets," *IEEE Transactions on Signal Processing*, vol. 51, no. 3, pp. 602–613, Mar. 2003.

[9] A. N. T. Pham and Y. Liang, "Joint channel and frequency offset estimation in distributed MIMO flat-fading channels," *IEEE Transactions on Wireless Communications*, vol. 7, no. 2, pp. 648–656, Feb. 2008.
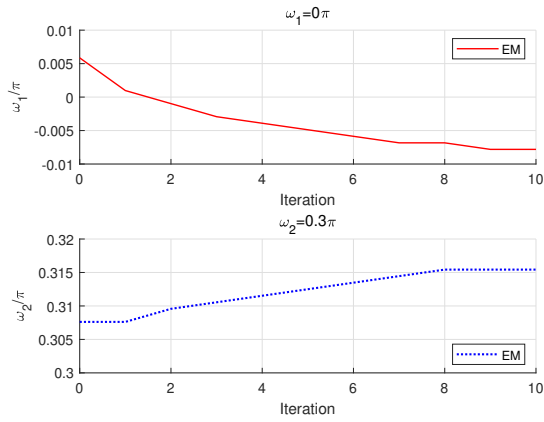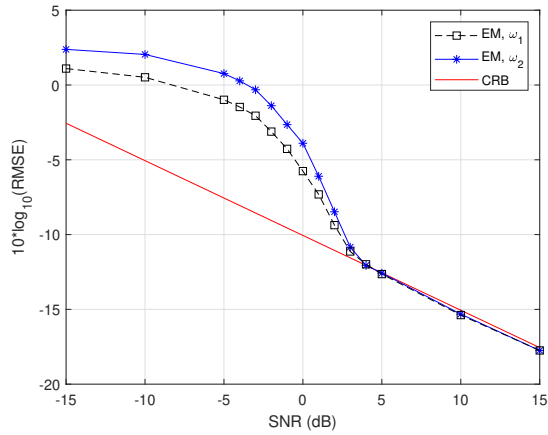
Fig. 9. Estimation algorithm convergence.

Fig. 10. frequency offset estimation Root Mean Square Error (RMSE) versus SNR under $\Delta\theta = \angle(\Upsilon_{1,2}) \pm \pi$, $N = 10$, $\Delta w = 0.3\pi$.

[10] S. M. J. Chen, Y. Wu and T. Ng, "Joint CFO and channel estimation for multiuser MIMO-OFDM systems with optimal training sequences," *IEEE Transactions on Signal Processing*, vol. 56, no. 8, pp. 4008–4019, Aug. 2008.

[11] W. Z. H. Abdzadeh-Ziabari and M. N. S. Swamy, "Joint carrier frequency offset and doubly selective channel estimation for MIMO-OFDMA uplink with Kalman and particle filtering," *IEEE Transactions on Signal Processing*, vol. 66, no. 15, pp. 4001–4012, Aug. 2018.

[12] P. Priya and D. Sen, "Particle filter based nonlinear data detection in presence of CFO for frequency selective mmWave MIMO-OFDM systems," *IEEE Transactions on Vehicular Technology*, vol. 70, no. 6, pp. 5892–5907, Jun. 2021.

[13] N. J. Myers and R. W. Heath, "Message passing-based joint CFO and channel estimation in mmWave systems with one-bit adcs," *IEEE Transactions on Wireless Communications*, vol. 18, no. 6, pp. 3064–3077, Jun. 2019.

[14] X. L. X. Yang, W. T. Shih and S. Jin, "Millimeter wave compressive path tracking with carrier frequency offset," in *2019 IEEE Wireless Communications and Networking Conference (WCNC)*, 2019, pp. 1–6.

[15] H. L. V. Trees, K. L. Bell, and Z. Tian, *Detection, Estimation, and Modulation Theory, Part I: Detection, Estimation, and Filtering Theory*, 2nd ed. Wiley, 2014.